Molecular Biology of the Cell
Vol. 17, 4167–4178 October 2006

Fta2, an Essential Fission Yeast Kinetochore Component, Interacts Closely with the Conserved Mal2 Protein[D]

Anne Kerres,* Visnja Jakopec,* Christoph Beuter,* Inga Karig,* Jennifer Pöhlmann,* Alison Pidoux,† Robin Allshire,† and Ursula Fleig*

*Lehrstuhl für funktionelle Genomforschung der Mikroorganismen, Heinrich-Heine Universität, 40225 Düsseldorf, Germany; and †Wellcome Trust Centre for Cell Biology, Institute of Cell and Molecular Biology, University of Edinburgh, Edinburgh EH9 3JR, United Kingdom

Submitted April 4, 2006; Revised June 26, 2006; Accepted July 11, 2006
Monitoring Editor: Ted Salmon

The fission yeast multiprotein-component Sim4 complex plays a fundamental role in the assembly of a functional kinetochore. It affects centromere association of the histone H3 variant CENP-A as well as kinetochore association of the DASH complex. Here, multicopy suppressor analysis of a mutant version of the Sim4 complex component Mal2 identified the essential Fta2 kinetochore protein, which is required for bipolar chromosome attachment. Kinetochore localization of Mal2 and Fta2 depends on each other, and overexpression of one protein can rescue the phenotype of the mutant version of the other protein. *fta2 mal2* double mutants were inviable, implying that the two proteins have an overlapping function. This close interaction with Fta2 is not shared by other Sim4 complex components, indicating the existence of functional subgroups within this complex. The Sim4 complex seems to be assembled in a hierarchical way, because Fta2 is localized correctly in a *sim4* mutant. However, Fta2 kinetochore localization is reduced in a *spc7* mutant. Spc7, a suppressor of the EB1 family member Mal3, is part of the conserved Ndc80–MIND–Spc7 kinetochore complex.

INTRODUCTION

The segregation of the duplicated sister chromatids into two equal sets is achieved by the interaction between spindle microtubules and chromosomes. Attachment of the mitotic spindle fibers occurs at the kinetochore, a multicomponent organelle assembled on centromeric DNA. Kinetochores perform various functions during mitosis: they mediate attachment of the sister chromatids with the plus-ends of spindle microtubules and maintain microtubule attachment during dynamic microtubule behavior, thus generating the physical forces required for chromosome movement. In addition, this complex is needed for spindle checkpoint signaling that regulates anaphase onset. These functions can be carried out by essentially all types of kinetochores, although the centromeric DNA requirements and the composition of the various protein kinetochore complexes can vary greatly between different organisms (Pidoux and Allshire, 2000; Cleveland *et al*., 2003).

The simplest kinetochore seems to be that of the budding yeast *Saccharomyces cerevisiae*, which consists of 125-base pair centromeric DNA and >60 kinetochore proteins organized into discrete complexes (De Wulf *et al*., 2003; McAinsh *et al*., 2003; Westermann *et al*., 2003). Budding yeast kinetochores exist during most of the cell cycle, and the proteins of this organelle are organized into multiple functional subcomplexes that are assembled hierarchically. The outer part of the budding yeast kinetochore associates with a single spindle microtubule (Winey *et al*., 1995).

Kinetochores from higher eucaryotes, in contrast, can encompass megabases of highly repetitive DNA sequences, they are predicted to contain >100 proteins, and they are assembled from S phase to early mitosis (Fukagawa, 2004; Maiato *et al*., 2004). The association of ~20 microtubule plus-ends to the outer plate of a vertebrate kinetochore requires correct orientation of the microtubule attachment sites to one pole to avoid merotelic attachments.

The kinetochores of the fission yeast *Schizosaccharomyces pombe* lie in between these two extremes. The centromeric DNA of *S. pombe* is 35–100 kb and is composed of a central core region that is flanked by inner and outer repetitive sequences. Marker genes that are placed within the centromeric DNA are transcriptionally silenced (Allshire *et al*., 1994, 1995). *S. pombe* kinetochore proteins identified to date either associate with the central domain or with the heterochromatic outer repeats, thus enforcing the existence of two distinct domains in the fission yeast centromeres. Although the outer repeats play an important role in sister centromere cohesion and possibly help to properly orient the multiple kinetochore microtubule attachment sites (Pidoux and Allshire, 2004), the central region is needed for the assembly of the kinetochore per se and the interaction with the mitotic spindle fibers (Saitoh *et al*., 1997; Goshima *et al*., 1999; Jin *et al*., 2002; Pidoux *et al*., 2003; Kerres *et al*., 2004; Obuse *et al*., 2004; Liu *et al*., 2005; Sanchez-Perez *et al*., 2005). The central region has a distinct composition as evidenced by the association of the conserved histone H3 variant Cnp1 and shows an unusual chromatin structure, because a limited micrococcal nuclease digestion gives rise to a smear instead of the expected nucleosomal ladder (Polizzi and Clarke, 1991; Takahashi *et al*., 1992, 2000). Kinetochore proteins that associate with the central region are required to maintain this specialized chromatin structure (Saitoh *et al*.,

This article was published online ahead of print in *MBC in Press* (http://www.molbiolcell.org/cgi/doi/10.1091/mbc.E06–04–0264) on July 19, 2006.

[D] The online version of this article contains supplemental material at *MBC Online* (http://www.molbiolcell.org).

Address correspondence to: Ursula Fleig (fleigu@uni-duesseldorf.de).

1997; Goshima *et al.*, 1999; Jin *et al.*, 2002). A substantial number of proteins that associate constitutively with the central region have been described, and mutations in genes coding for these proteins lead to extreme missegregation of chromosomes (Saitoh *et al.*, 1997; Goshima *et al.*, 1999; Jin *et al.*, 2002; Pidoux *et al.*, 2003; Hayashi *et al.*, 2004). Recently, using affinity purification, the majority of these proteins have been grouped into two biochemically separable complexes, namely, the Ndc80–MIND–Spc7 and the Sim4 complexes (Liu *et al.*, 2005). The MIND complex, made up of four conserved, essential proteins, serves in budding yeast as a bridge between kinetochore subunits that associate with the centromeric DNA and those that bind microtubules (De Wulf *et al.*, 2003; Obuse *et al.*, 2004). The four component Ndc80 complex is also conserved from yeast to human and is required for kinetochore–microtubule association and spindle checkpoint signaling (He *et al.*, 2001; Janke *et al.*, 2001; Wigge and Kilmartin, 2001). Finally, the Spc7 protein was identified as an interaction partner of the Mal3 protein, a member of the EB1 family of microtubule plus-end–binding proteins (Kerres *et al.*, 2004). Its *Caenorhabditis elegans* homologue KNL-1 is required for targeting a number of components of the outer kinetochore, thus directing the assembly of the microtubule–kinetochore interface (Desai *et al.*, 2003). Proteins of the Ndc80–MIND–Spc7 complex have been shown to be required for the special chromatin structure of the central centromere region; however, they do not seem to be required for the association of the kinetochore-specific histone H3 variant Cnp1 with this region (Goshima *et al.*, 1999; Takahashi *et al.*, 2000; Hayashi *et al.*, 2004). This is in contrast to Sim4 complex components, which affect the chromatin structure and incorporation of Cnp1 (Takahashi *et al.*, 2000; Pidoux *et al.*, 2003). The Sim4 complex consists of 13 proteins: the previously identified Sim4, Mis6, Mal2, Mis15, and Mis17 proteins as well as the newly identified Fta1-7 proteins and Dad1, a component of the DASH complex (Saitoh *et al.*, 1997; Jin *et al.*, 2002; Pidoux *et al.*, 2003; Hayashi *et al.*, 2004; Liu *et al.*, 2005; Sanchez-Perez *et al.*, 2005). Interestingly, one of the functions of the Sim4 complex is to act as a loading dock for the transient association of the nonessential fission yeast DASH complex with the kinetochore. It thus plays a role in chromosome biorientation (Liu *et al.*, 2005; Sanchez-Perez *et al.*, 2005). To better understand the function of the Sim4 complex in mitosis, we conducted a screen for extragenic suppressors of one of its members, namely, the Mal2 protein (Fleig *et al.*, 1996; Jin *et al.*, 2002). Mal2 is a conserved kinetochore component that is essential for faithful chromosome segregation. Its budding yeast counterpart, the Mcm21 protein, is part of the four-component COMA complex, that links DNA-associated kinetochore subcomplexes with those associating with microtubules (Ortiz *et al.*, 1999; De Wulf *et al.*, 2003). However, the other members of the COMA complex do not seem to exist in fission yeast. Recently, orthologues of Mal2 have been identified by computational approaches in a large number of eucaryotes (Meraldi *et al.*, 2006). Furthermore, the human Mal2 homologue CENP-O was isolated in screens that identified proteins associated with centromeric chromatin, pointing to the importance of this protein in kinetochore function (Foltz *et al.*, 2006; Okada *et al.*, 2006) In this study, we identified Fta2 as a close interaction partner of Mal2 and provide evidence that the Sim4 complex seems to be assembled in a hierarchical way.

MATERIALS AND METHODS

Strains and Media

Yeast strains used in this study are listed in Table 1. New strains were obtained by crossing the appropriate strains followed by tetrad or random spore analysis and genotyping. At least three double mutants were tested per cross. Strains were grown in rich media (YE5S) or minimal media (EMM or MM) with the required supplements (Moreno *et al.*, 1991). MM with 5 μg/ml thiamine repressed the *nmt* promoters. For high-level expression from *nmt* promoters, cells were grown in thiamine-less media for 22–24 h at 25°C or for 18–20 h at 30°C. Resistance to G418 was tested on YE5S plates containing 100 mg/l G418. Transcriptional silencing assays were carried out as described previously (Jin *et al.*, 2002; Pidoux *et al.*, 2003).

Identification of *fta2*$^+$ and DNA Methods

Multicopy extragenic suppressors of the *mal2-1* temperature-sensitive (ts) phenotype were isolated by transformation of this strain with a genomic *S. pombe* DNA bank (Barbet *et al.*, 1992). Ura$^+$ transformants were isolated at 30.5°C to 32°C, and the genomic DNA inserts of the plasmids were sequenced. At 32°C, only wild-type *mal2*$^+$ could be isolated. At 30.5°C, 4/15,000 transformants showed better growth. The plasmids of transformants able to grow better at 30.5°C but not at higher temperatures were analyzed further. One plasmid that contained four open reading frames (ORFs) (cosmid c1783 position, 739-6205) was subcloned to determine which ORF suppressed the *mal2-1* ts phenotype. This identified the ORF with the systematic name SPAC1783.03, which has recently be named *fta2*$^+$ (Liu *et al.*, 2005).

A *fta2*$^+$ null allele (Δ*fta2*$^+$) was generated by replacing the entire 1056 base pairs of the *fta2*$^+$ ORF plus seven base pairs of the 3′ noncoding region with the Kanamycin-resistance (Kan^R) cassette in diploid strain KG425 × KG554 (Bahler *et al.*, 1998). Tetrad analysis of 77 heterozygous Δ*fta2*$^+$/*fta2*$^+$ diploids revealed that only the two kanamycin-sensitive (Kan^S) spores/tetrad grew. We attempted to delete the *mal2*$^+$ ORF in haploid strain KG425 overexpressing *fta2*$^+$ from the *nmt1*$^+$ promoter as described previously (Fleig *et al.*, 1996). We generated endogenous *fta2*$^+$-*gfp*, *fta2*$^+$-HA, *mal2-1-gfp* fusions via polymerase chain reaction (PCR)-based gene targeting by using the Kan^R cassette (Bahler *et al.*, 1998). The correct Kan^R transformants were indistinguishable in phenotype from the isogenic parental strain.

Generation of *fta2*^{ts} Alleles

A pBSK-based plasmid containing the entire 1056-base pair-long *fta2*$^+$ ORF followed 3′ by the *his3*$^+$ gene was used as a template for a mutagenic PCR reaction that amplified the 3256-base pair-long *fta2*$^+$ *his3*$^+$ DNA fragment. This fragment was transformed in strain UFY 819, which contained the *ura4*$^+$ marker placed behind the genomic *fta2*$^+$ gene. His$^+$ transformants that grew at 25°C but not at 36°C were identified and tested for loss of the *ura4*$^+$ marker on 5-fluoroorotic acid. Correct integration of the mutagenized DNA fragments was tested via PCR. A *fta2*$^+$ containing plasmid was able to fully rescue the temperature sensitivity of these mutant strains, which were backcrossed twice.

Immunoprecipitations

Chromatin immunoprecipitations (ChIP) were performed as described previously (Pidoux *et al.*, 2003; Kerres *et al.*, 2004). We performed at least three independent ChIP analyses per strain and temperature.

For coimmunoprecipitation, Fta2-HA–, Mal2-GFP–, and Fta2-HA Mal2-GFP–expressing strains were grown at 30°C in YE5S over night followed by protein extraction and immunoprecipitation as has been described previously (Kerres *et al.*, 2004). Eluates were boiled and resolved on a SDS-9% polyacrylamide gel and blotted. Blots were probed with anti-hemagglutinin (HA) antibody (monoclonal mouse; Roche Diagnostics, Mannheim. Germany) followed by the secondary antibody (peroxidase-conjugated AffiniPure goat anti-mouse IgG [H+L]; Jackson ImmunoResearch Laboratories, West Grove, PA). Immobilized antigens were detected using the ECL Advance Western blotting kit (GE Healthcare, Little Chalfont, Buckinghamshire, United Kingdom).

Microscopy

Photomicrographs were obtained with a Zeiss Axiovert200 fluorescence microscope (Carl Zeiss, Jena, Germany) coupled to a charge-coupled device camera (Orca-ER; Hamamatsu, Bridgewater, NJ) and Openlab imaging software (Improvision, Coventry, United Kingdom). Immunofluorescence microscopy was done as described previously (Hagan and Hyams, 1988; Bridge *et al.*, 1998). Tubulin was stained using monoclonal anti-TAT1 antibodies followed by fluorescein isothiocyanate-conjugated goat anti-mouse antibodies (Sigma-Aldrich, St. Louis, MO). HA or green fluorescent protein (GFP) fusion proteins were observed in fixed cells by indirect immunofluorescence with mouse anti-HA antibody (Covance, Princeton, NJ) or rabbit anti-GFP antibodies (Invitrogen, Carlsbad, CA), respectively. Cy3-conjugated sheep anti-mouse antibodies or Cy3-conjugated sheep anti-rabbit antibodies (Sigma-Aldrich) were used as secondary antibodies. Cells were stained with 4,6-diamidino-2-phenylindole (DAPI) before mounting.

RESULTS

Identification of *fta2*$^+$ as a Suppressor of the *mal2-1* ts Mutant Phenotype

The conditionally lethal ts *mal2-1* allele leads to severe missegregation of endogenous chromosomes at the restrictive tem-

Table 1. Yeast strains used in this study

Name	Genotype	Source
UFY819	*h+ fta2+/ura4+ his3Δ leu1-32 ura4-D18 ade6-M210*	This study
UFY547	*h− mal2-1-GFP/KanR leu1-32 ade6-M210 ura4-D18*	This study
UFY518	*h− fta2-GFP/KanR leu1-32 ade6-M210 ura4-D6*	This study
UFY544	*h− fta2-GFP/KanR mal2-1 leu1-32 ade6-M210 ura4-D18*	This study
UFY1215	*h+ fta2-292/his3+ cnt1(NcoI):arg3+ cnt3(NcoI):ade6+ otr2(HindIII):ura4+ leu1-32 ura4-D18 arg3− ade6-M210*	This study
UFY1189	*h− fta2-292/his3+ imr1R(NcoI):ura4+ ade6-M210 leu1-32 ura4−*	This study
UFY1048	*h− fta2-291/his3+ his3− leu1-32 ura4-D18 ade6-M210*	This study
UFY1050	*h− fta2-292/his3+ his3− leu1-32 ura4-D18 ade6-M210*	This study
UFY1144	*h+ fta2-291/his3+ his7+::lacI-GFP lys1+::LacOP ura4− leu1-32*	This study
UFY1179	*h+ fta2-291/his3+ mad2Δ::ura4+ ura4-D18 ade6-M210 leu1-32*	This study
UFY1180	*h+ fta2-291/his3+ mph1Δ::ura4+ ura4-D18 ade6-M210 leu1-32*	This study
UFY1124	*h− fta2-292/his3+ mal2-GFP/KanR ade6-M210 leu1-32 ura4− his3−*	This study
UFY787	*h− fta2-HA/KanR his3-D1 ade6-M210 leu1-32 ura4-D18*	This study
UFY789	*h+ fta2-HA/KanR mal2-GFP/KanR ura4− leu1-32 ade6-M210*	This study
UFY1202	*h+ fta2-291/his3+ mis15-68 leu1-32 ura4-D18*	This study
UFY1204	*h− fta2-292/his3+ mis15-68 leu1-32*	This study
UFY1198	*h− fta2-291/his3+ mis6-302 leu1-32 ade6-M210*	This study
UFY1200	*h+ fta2-292/his3+ mis6-302 leu1-32*	This study
UFY1219	*h+ fta2-291/his3+ sim4-193 leu1-32 his3-D1 ura4-D18 ade6-M210*	This study
UFY886	*h+ fta2-GFP/KanR sim4-193 ade6-M210 leu1-32 ura4−*	This study
UFY889	*h− fta2-GFP/KanR mis6-302 leu1-32*	This study
UFY1131	*h+ fta2-GFP/KanR mis15-68 leu1-32*	This study
UFY1129	*h− fta2-GFP/KanR mis17-362 leu1-32 ura4-D6*	This study
UFY1211	*h− fta2-291/his3+ sim4-GFP/KanR his3-D1 leu1-32 ade6-M210 ura4−*	This study
UFY1239	*h− fta2-291/his3+ mis6-3HA::leu+ ade6-M210 leu1-32 ura4−*	This study
UFY1054	*h− fta2-292/his3+ dad1-GFP/KanR leu1-32 ura4-D18 ade6-M210*	This study
UFY885	*h+ fta2-GFP/KanR mis12-537 leu1-32 ade6-M210*	This study
UFY1184	*h+ fta2-GFP/KanR nuf2-1::ura4+ ura4− leu1-32*	This study
UFY1028	*h+ spc7-23/his3+ his3-D1 ade6-M216 leu1-32 ura4-D18*	This study
UFY1170	*h+ fta2-GFP/KanR spc7-23/his3+ leu1-32 ade6-M210 ura4−*	This study
UFY1237	*h− fta2-291/his3+ spc7-GFP/KanR ade6-M210 ura4−*	This study
UFY1085	*h− fta2-291/his3+ spc7-23/his3+ leu1-32 ade6-M210 ura4-D18 his3-D1*	This study
UFY852	*h− mal2-1 leu1-32 ade6-M210 ura4-D18*	U. Fleig
UFY597	*h+ mal2-GFP/KanR ade6-M210 leu1-32 ura4-D6*	U. Fleig
FY3027	*h+ cnt1(NcoI):arg3 cnt3(NcoI):ade6 otr2(HindIII):ura4 tel1L:his3 ade6-M210 leu1-32 ura4-D18 arg3-D4 his3-D1*	R. Allshire
FY4540	*h− sim4-193 cnt1(NcoI):arg3 cnt3(NcoI):ade6 otr2(HindIII):ura4 tel1L:his3 ade6-M210 leu1-32 ura4-D18 arg3-D4 his3-D1*	R. Allshire
FY5231	*h+ sim4-193 arg3-D4 ade6-M210 his3-D1 ura4-D18 leu1-32*	R. Allshire
KG425	*h− ade6-M210 leu1-32 his3Δ ura4-D18*	K. Gould
KG554	*h+ ade6-M216 leu1-32 his3Δ ura4-D18*	K. Gould
ANF251-9A	*h+ nuf2-1::ura4+ ura4-D18*	Y. Hiraoka
SS638	*h− mad2Δ::ura4+ leu1-32 ura4-D18 ade6-M210*	S. Sazer
SS560	*h− mph1Δ::ura4+ leu1-32 ura4-D18 ade6-M216*	S. Sazer
	h− mis6-302 leu1-32	M. Yanagida
	h− mis15-68	M. Yanagida
	h− mis17-362	M. Yanagida
	h− mis12-537 leu1-32	M. Yanagida

perature (Fleig *et al*., 1996; Jin *et al*., 2002). To identify Mal2 interaction partners, we conducted a multicopy extragenic suppressor screen and identified an ORF with the systematic name SPAC1783.03 that was able to suppress the temperature sensitivity of the *mal2-1* strain (see *Materials and Methods*; Figure 1A). SPAC1783.03 codes for a 40.5-kDa protein that shows no strong sequence similarity to other proteins in the databases (Sanger Institute, Cambridge, United Kingdom). Recently, this ORF was named *fta2*+ (Liu *et al*., 2005). *fta2*+ driven by its own promoter on plasmid pUR19 rescued the ts phenotype of the *mal2-1* strain up to 32°C, whereas overexpression of *fta2*+ from the repressible, wild-type *nmt1*+ promoter resulted in suppression of the *mal2-1* nongrowth phenotype at all temperatures tested (Figure 1A). We next tested whether the essential *mal2*+ ORF could be replaced by high level *fta2*+ expression. To this end we attempted, but failed, to delete the *mal2*+ ORF in haploid strains strongly overexpressing *fta2*+ (see *Materials and Methods*).

The suppression of the *mal2-1* ts phenotype by *fta2*+ is due to suppression of the chromosome missegregation observed in *mal2-1* cells; 53.5% of *mal2-1* anaphase cells transformed with a vector control and incubated at the nonpermissive temperature for 6 h showed severe chromosome segregation defects. This phenotype was fully suppressed by the presence of wild-type *mal2*+ on a plasmid and reduced to 9.2% in *mal2-1* cells expressing extra *fta2*+ (Figure 1B).

As shown by the immunofluorescence analysis of a Mal2-1-GFP fusion protein, the mutant Mal2-1 protein is present at the kinetochore at 25°C. However, Mal2-1 kinetochore association is not observed at the restrictive temperature (Figure 1C). Overexpression of *fta2*+ in this strain rescues this phenotype, because Mal2-1-GFP shows kinetochore association at the restric-

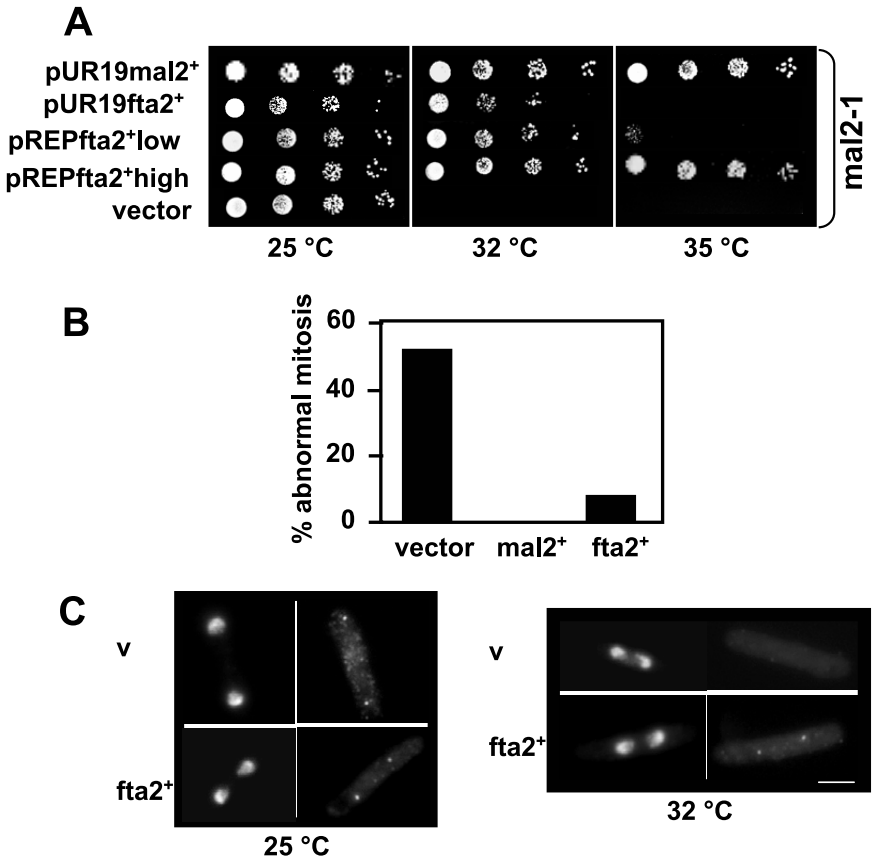

Figure 1. *fta2*$^+$ suppresses the phenotypes of the *mal2-1* mutant strain. (A) The rescue of the *mal2-1* ts phenotype by *fta2*$^+$ is dosage dependent. Serial dilution patch tests (10^4 to 10^1 cells) of *mal2-1* transformants grown under selective conditions at the indicated temperatures for 4–6 d. Vector control indicates plasmid without insert; pUR19mal2$^+$ and pUR19fta2$^+$ denotes the presence of wild-type *mal2*$^+$ or *fta2*$^+$ expressed by their endogenous promoters on plasmid pUR19. pREPfta2$^+$low and pREPfta2$^+$high denote presence of wild-type *fta2*$^+$ driven by the *nmt1* promoter under repressed (low) or derepressed (high) conditions, respectively. (B) Overexpression of *fta2*$^+$ suppresses mitotic defects in *mal2-1* cells. The number of abnormal mitosis was determined in *mal2-1* cells transformed with a vector control or plasmids expressing wild-type *mal2*$^+$ or *fta2*$^+$. Cells were shifted from 25 to 32°C for 6 h, fixed, and the number of aberrant anaphases was determined. N/strain = 50. (C) Kinetochore localization of Mal2-1-GFP is dependent on *fta2*$^+$ overexpression. *mal2-1-gfp* cells transformed with vector control (v) or a plasmid expressing *fta2*$^+$ under the control of the *nmt1*$^+$ promoter were grown at 25 or 36°C for 6 h, and the localization of Mal2-1-GFP was determined. Bar, 5 μm.

tive temperature in the presence of extra *fta2*$^+$ (Figure 1C). We conclude that extra *fta2*$^+$ is able to rescue the *mal2-1* strain by stabilizing the mutant Mal2-1 protein and/or by helping the mutant Mal2-1 protein to associate with the kinetochore at the nonpermissive temperature.

Association of the Essential Fta2 Protein with the Kinetochore Is Dependent on the Presence of Functional Mal2

To determine whether *fta2*$^+$ was essential for vegetative growth one copy of the *fta2*$^+$ ORF was replaced with the Kan^R (kanamycin resistance) marker in a diploid strain (see *Materials and Methods*). Sporulation followed by tetrad analysis of 77 tetrads of this strain revealed that only two of the four spores in a tetrad could grow, and these were kanamycin sensitive, indicating that *fta2*$^+$ is an essential gene. To determine the subcellular localization of Fta2, a fluorescence-improved version of GFP was fused to the COOH-terminal end of the endogenous *fta2*$^+$ ORF (see *Materials and Methods*). Immunofluorescence of interphase and mitotic cells revealed a localization pattern characteristic of *S. pombe* kinetochore proteins, namely, a single fluorescent dot near the nuclear periphery in interphase and late mitotic cells and up to six fluorescent dots in metaphase cells (Figure 2A) (Jin *et al*., 2002). This localization pattern is dependent on the presence of a functional Mal2 protein, because no specific Fta2-GFP signal could be detected in a *mal2-1* strain incubated at the restrictive temperature (Figure 2B). Fta2 protein levels in the cell were not affected in the *mal2-1* strain (Supplemental Figure 1). To identify the centromere region with which Fta2 associates and to determine whether the association of Fta2-GFP with centromeric DNA was dependent on Mal2, ChIP was carried out (Partridge *et al*., 2000). Wild-type or *mal2-1* cells expressing Fta2-GFP were analyzed in ChIP assays by using anti-GFP antibodies. The DNA present in crude extracts or in the immunoprecipitates was analyzed by multiplex PCR analysis using primers to amplify the *cnt*, *imr*, and *otr* regions of centromere I and an unrelated euchromatic control (*fbp*) (Figure 2C). In wild-type cells, Fta2 associates with the central centromere region as shown by the specific enrichment of the *cnt* and *imr* sequences in the Fta2-GFP ChIP (Figure 2C) (Liu *et al*., 2005). In *mal2-1* cells, Fta2 ChIPs also showed enrichment of the *cnt* and *imr* sequences at the permissive temperature (25°C); however, incubation at the nonpermissive temperature led to a severe reduction of the *cnt* and *imr* sequences brought down by ChIP (Figure 2C). These data imply that Fta2 localization at the kinetochore was dependent on Mal2.

Because mutations in genes encoding components of the kinetochore affect centromeric silencing (Pidoux and Allshire, 2000), we tested whether marker genes placed within the centromere DNA were still transcriptionally repressed in the *fta2-292* ts mutant strain (see below). To this end, we assayed growth of *fta2-292* strains that had the *ura4*$^+$ marker gene inserted at *otr2* (otr region of centromere 2) or *imr1*, or the *arg3*$^+$ marker gene inserted at *cnt1* (Partridge *et al*., 2000; Pidoux *et al*., 2003). Wild-type strains carrying a marker gene inserted at a centromeric region are auxotroph for that particular marker due to transcriptional repression of the centromeric DNA (Pidoux and Allshire, 2000). The presence of *fta2-292* had no influence on transcriptional silencing of the *otr* and *imr* regions but led to alleviation of silencing at the central *cnt* region (our unpublished data; Figure 2D). Wild-type strains containing the promoter-crippled *arg3*$^+$ gene inserted into the *cnt1* region

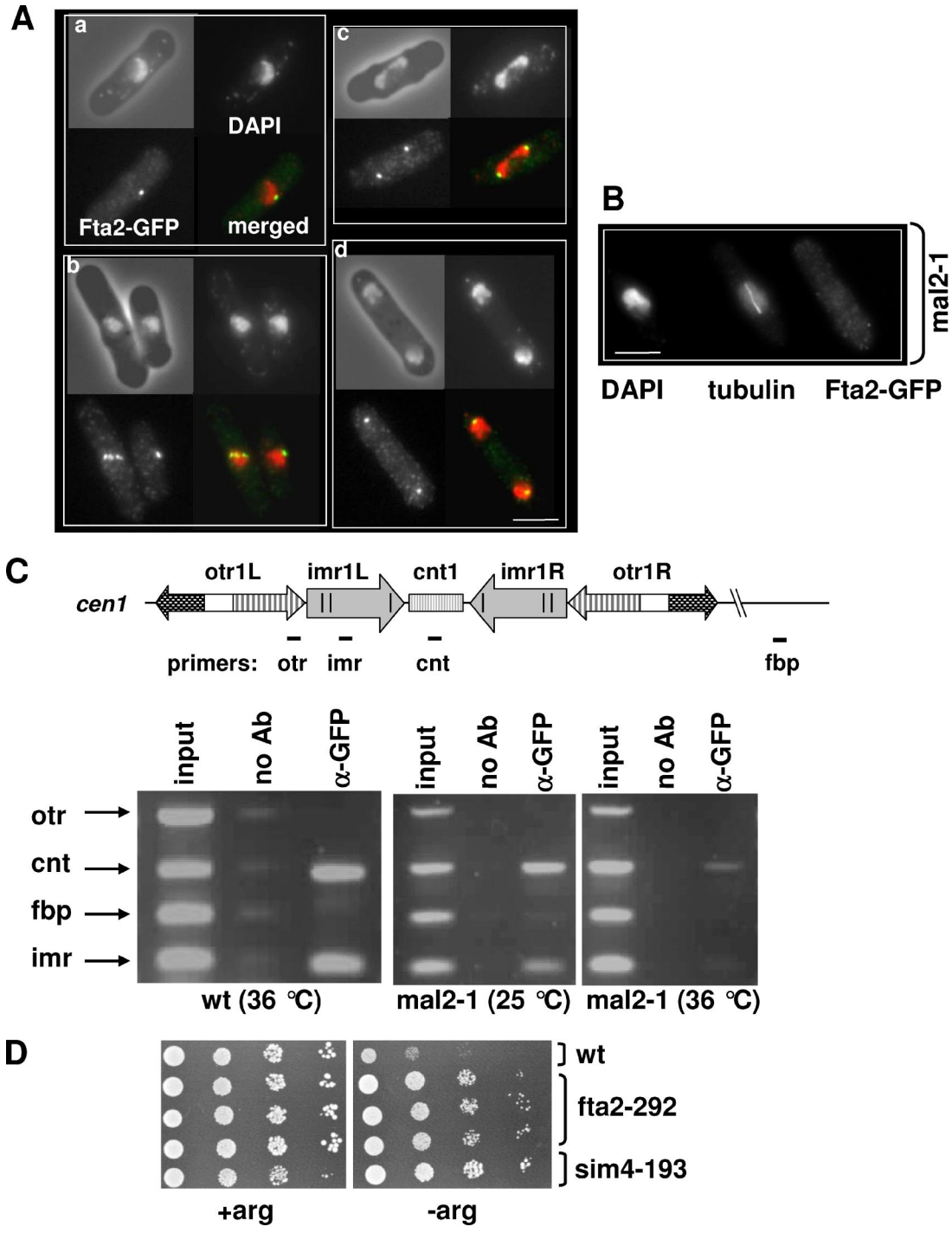

Figure 2. Fta2 kinetochore localization is dependent on functional Mal2. (A) Localization of the Fta2-GFP protein in wild-type cells in interphase (a) and early, middle, and late mitosis (b [left cell]–d, respectively). Fixed cells were stained with DAPI and anti-GFP antibody. Bar, 5 μm. (B) Localization of Fta2-GFP in an early mitotic *mal2-1* cell. Cells were incubated for 6 h at 36°C, fixed, and stained with DAPI, anti-tubulin antibody, and anti-GFP antibody. Bar, 5 μm. (C) Fta2 association with the central domain of *cen1* is Mal2 dependent. Wild-type or *mal2-1* cells expressing Fta2-GFP were fixed and processed for ChIP by using anti-GFP antibodies. The chromatin in immunoprecipitates and in the crude extracts was analyzed by multiplex PCR. The amplified regions in *cen1* are indicated. *fbp*, euchromatic negative control. The *cnt* and *imr* regions are enriched in Fta2-GFP ChIPs from wild-type cells; the association of Fta2-GFP with these regions is reduced or severely reduced in *mal2-1* cells grown at 25 or 36°C (for 6 h), respectively. (D) Fta2 is involved in *cnt* centromeric silencing. Serial dilution patch tests (10^4 to 10^1 cells) of wild-type, *fta2-292*, and *sim4-193* cells that have the *arg3*$^+$ gene inserted at *cnt1*. Alleviation of silencing leads to growth on arginine minus (−arg) plates. Cells were incubated at 30°C for 5 d.

grow very poorly on medium that does not contain arginine, whereas kinetochore mutants such as *sim4-193* alleviate *cnt1* silencing and allow fast growth on arginine minus medium (Figure 2D) (Pidoux *et al.*, 2003). The presence of the mutant

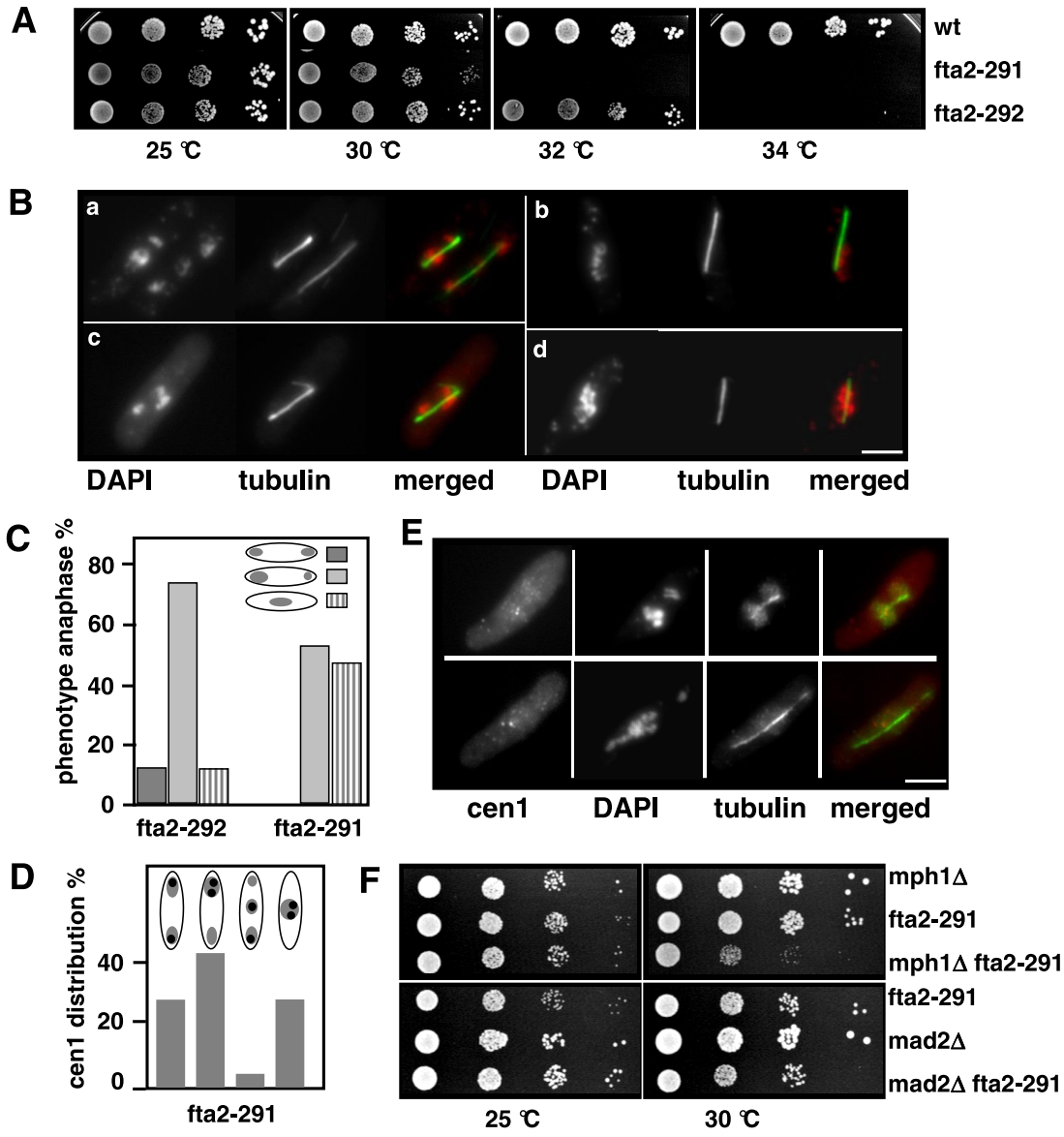

Figure 3. ts *fta2* mutants have severe mitotic defects. (A) Serial dilution patch tests (10^4 to 10^1 cells) of wild-type (wt), *fta2-291*, and *fta2-292* strains grown at the indicated temperatures for 3 d. (B) Photomicrographs of mitotic *fta2-291* (a and b) and *fta2-292* (c and d) cells incubated for 6 h at 36°C. Fixed cells were stained with DAPI and anti-tubulin antibody. Shown are the main two phenotypes: unequally/partially segregated (a and c) or nonseparated (b and d) chromatin on an elongating spindle. (C) Diagrammatic representation of anaphases observed in *fta2-291* and *fta2-292* strains incubated for 6 h at 36°C. N/strain = 60. (D) Diagrammatic representation of *cen1* distribution in mitotic *fta2-291* cells with an elongating spindle (cen1 signal, black dot). (E) Distribution of GFP-marked *cen1* in mitotic *fta2-291* cells. Cells were incubated for 6 h at 36°C, fixed, and stained with anti-GFP antibody, DAPI, and anti-tubulin antibody. (F) *fta2-291* interacts genetically with a component of the spindle checkpoint pathway. Serial dilution patch tests of *mph1*Δ, *mad2*Δ, *fta2-291* and the respective *fta2-291* double mutants grown at the indicated temperatures for 3 d.

fta2-292 allele led to good growth on medium without arginine implying that transcriptional silencing of the *cnt1* region has been alleviated (Figure 2D).

fta2 Mutants Show Severe Defects in Chromosome Segregation and Bipolar Attachment

To study the function of Fta2 in mitosis, we generated ts *fta2* alleles (see *Materials and Methods*). The two mutant *fta2* strains that showed the tightest ts phenotype were analyzed in greater detail. DNA sequence analysis revealed that both strains carried a single point mutation in the *fta2* ORF, one mutation at position 871 (G to A), and the other mutation at position 874 (T to C). The single base-pair changes resulted in single amino acid changes at position 291 (a change from glycine to serine) and position 292 (a change from phenylalanine to leucine) of the 351-amino acid-long Fta2 protein. The mutants were therefore named *fta2-291* and *fta2-292*, respectively (Figure 3A). Because the entire $fta2^+$ ORF was mutagenized but the two mutants with the most prominent ts phenotype had mutations in proximity to each other, we reasoned that the C-terminal region of Fta2 played an important role in its function. We therefore conducted another database search using WU-BLAST2 for putative Fta2 homologues using the last 81 C-terminal amino acids only

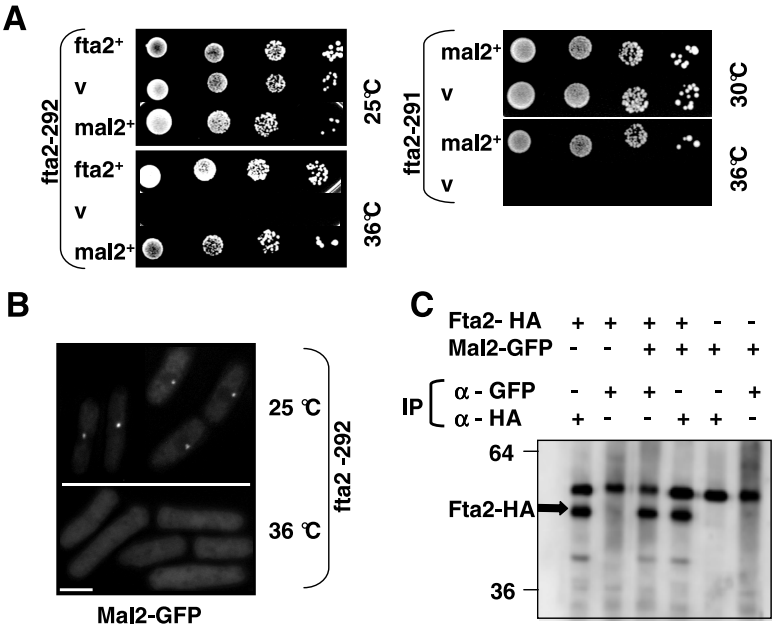

Figure 4. Extra *mal2*$^+$ suppresses the ts nongrowth phenotypes of the *fta2* mutant strains. (A) Serial dilution patch tests (10^4 to 10^1 cells) of *fta2-292* and *fta2-291* transformants grown under selective conditions at the indicated temperatures for 4 d. Vector control (v) indicates plasmid without insert; Mal2$^+$ denotes the presence of wild-type *mal2*$^+$ expressed by the endogenous promoters on plasmid pUR19 (for *fta2-292*) or from the thiamine-repressible *nmt1*$^+$ promoter in the absence of thiamine (for *fta2-291*). (B) Kinetochore localization of Mal2-GFP is abolished in the *fta2-292* strain at the nonpermissive temperature. *fta2-292* cells expressing Mal2-GFP were grown at 25°C or shifted for 6 h to 36°C and analyzed by fluorescence microscopy. (C) Coimmunoprecipitation of Fta2 and Mal2. Protein extracts from strains expressing Mal2-GFP, Fta2-HA, or both were used for immunoprecipitation (IP) with an anti-HA or anti-GFP antibody. The immunoprecipitates were resolved by SDS-PAGE and probed with an anti-HA antibody. Kilodalton size markers are indicated.

(Altschul *et al*., 1997). We found a very limited homology to the *S. cerevisiae* kinetochore protein Ctf13 (36% identical, 50% similar amino acids in a 63-amino acid-long region) (Supplemental Figure 2) (Doheny *et al*., 1993). Ctf13 is one of the four proteins of the CBF3 kinetochore complex, which is the essential centromere DNA binding complex in budding yeast (Doheny *et al*., 1993; Russell *et al*., 1999).

Interestingly, in this alignment the amino acids at position 291 and 292 of Fta2 were conserved (Supplemental Figure 2). However, at present it is unclear whether Ctf13 and Fta2 share a common domain.

To analyze the reason for the nongrowth phenotype of the *fta2* mutant strains at higher temperatures, *fta2-291* and *fta2-292* strains were incubated at the nonpermissive temperature for 6 h and analyzed by immunofluorescence. Although interphase cells showed no obvious abnormalities, mitotic cells were severely affected. All *fta2-291* mitotic cells and 86% of *fta2-292* mitotic cells showed severe chromosome segregation defects (Figure 3, B and C). The two predominant abnormal chromosome resolution phenotypes were 1) unequally or partially separated chromatin (Figure 3B, a and c) and 2) no separation of highly condensed chromatin on an elongating spindle (Figure 3B, b and d). The chromatin was separated, albeit unequally, in the majority of *fta2-292* mitotic cells, whereas nearly 50% of *fta2-291* mitotic cells were unable to separate their chromatin (Figure 3C). Aberrant spindle phenotypes were observed rarely. To further characterize the severe chromosome segregation defects observed in *fta2* mutant cells, we analyzed the segregation behavior of sister centromeres by monitoring the segregation behavior of centromere 1 marked with GFP (*cen1-gfp*) (Nabeshima *et al*., 1998). In interphase cells, the distribution of the cen1-GFP signals was very similar to that observed for wild-type cells, indicating that premature sister chromatid separation was not the cause of the aberrant chromatin distribution seen in *fta2* mutants. In mitotic cells, only 26.7% of *fta2-291* cells with an elongating spindle showed correct separation of *cen1* sister centromeres, although the chromatin in these cells was distributed unequally (Figure 3D). In 42.3% of cells, the sister centromeres segregated together, possibly due to syntelic microtubule attachment (Figure 3, D and E). In 3.8% of the cells, only one of the sister centromeres segregated to the end of the cell. Finally, in 26.7% of cells, sister chromatids were not segregated and remained in the middle of the cell (Figure 3D).

We next asked whether all centromeres were associated with the mitotic spindle by assaying colocalization of the cen1-GFP signal and the spindle (Figure 3E). We found that in cells with segregated chromatin 75% of cen1-GFP signals were spindle associated, whereas 25% were not. In cells with an elongating spindle but unseparated chromatin, the majority (58%) of cen1-GFP signals did not colocalize with the mitotic spindle. Our findings imply that the Fta2 protein is required for correct bipolar chromosome orientation and also plays a role in linking the kinetochore to spindle microtubules. The observed *fta2* mutant phenotypes should lead to activation of the spindle checkpoint.

This checkpoint regulates entry into anaphase by inhibiting the anaphase promoting complex until proper spindle microtubules association of the kinetochores. The absence of spindle microtubules will activate the attachment response, whereas the tension response will be activated in response to the absence of tension between sister kinetochores (Musacchio and Hardwick, 2002; Cleveland *et al*., 2003). We tested whether the spindle checkpoint was active in *fta2* mutant cells by constructing double mutants of *fta2-291* with null alleles of *mad2*$^+$ and *mph1*$^+$, which encode conserved components of the spindle checkpoint pathway (He *et al*., 1997, 1998). The growth properties of *mad2*Δ (*mad2*$^+$ deletion) *fta2-291* double mutants were indistinguishable from that of the single *fta2-291* mutant (Figure 3F). In contrast, *mph1*Δ *fta2-291* strains showed growth defects at 30°C (Figure 3F). We analyzed the phenotypic consequences of an *mph1*$^+$ deletion in *fta2-291* strain by incubation of the single and double mutants for 8 h at 30°C followed by DAPI staining. At this temperature, 47.1% of *fta2-291* anaphase cells showed aberrant chromosome segregation, whereas in the *mph1*Δ *fta2-291* double mutant, this number rose to 64.1% (our unpublished data). Our results indicate that the *mph1*$^+$ spindle checkpoint branch is required for survival of the *fta2-291* strain at 30°C.

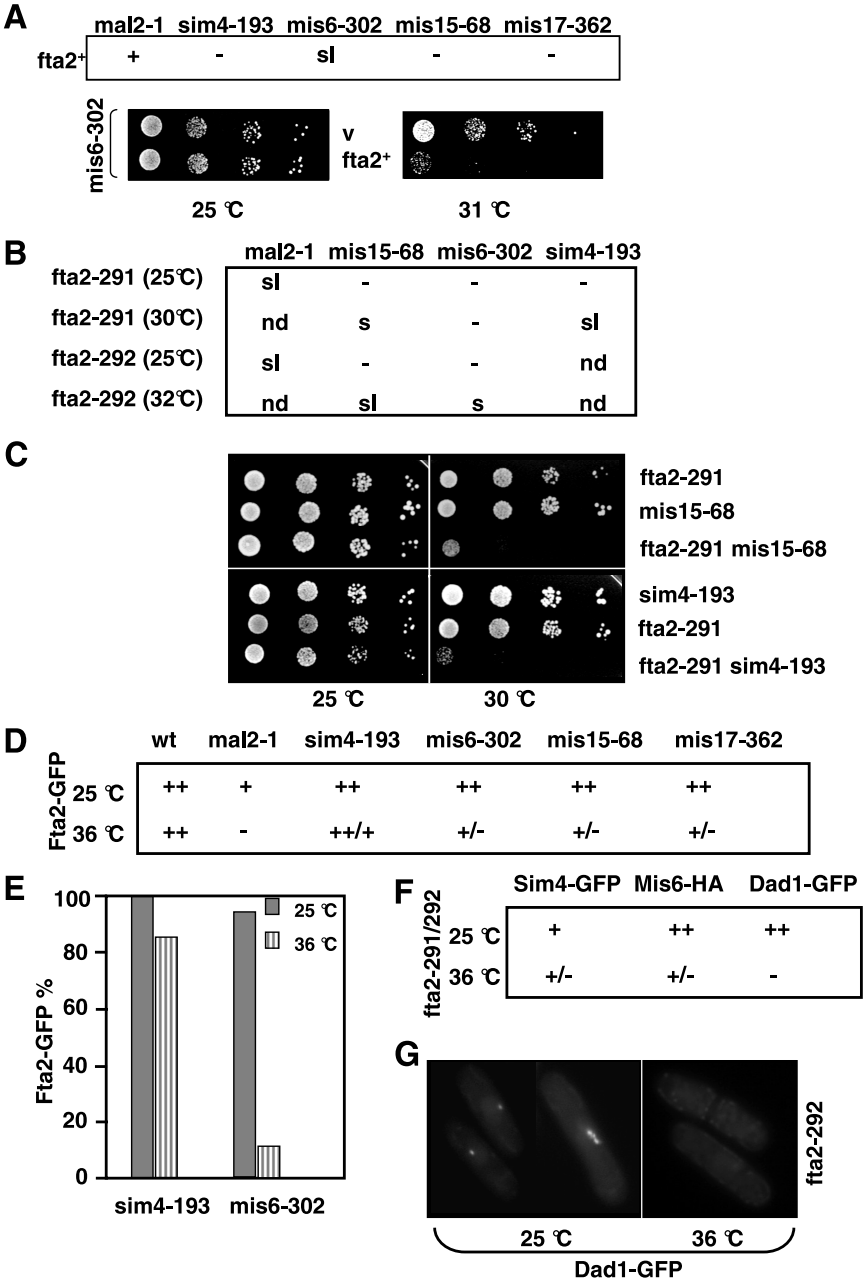

Figure 5. Interaction between *fta2*$^+$ and other components of the Sim4 kinetochore complex. (A) Plasmid-borne expression of *fta2*$^+$ from the *nmt1*$^+$ promoter rescues the ts phenotype of a *mal2-1* mutant (+), leads to synthetic lethality (sl) of a *mis6-302* mutant at the semipermissive temperature and has no effect (−) on the growth of the *sim4-193*, *mis15-68*, and *mis17-362* strains at temperatures below the restrictive temperature. Serial dilution patch tests of *mis6-302* transformants grown under selective conditions at the indicated temperatures for 4 d. v, vector control. (B) Growth of double mutants of *fta2-291* and/or *fta2-292* with other components of the Sim4 complex. sl, synthetic lethal; s, reduced growth; −, no effect; nd, not done. (C) Serial dilution patch tests of *fta2-291*, *mis15-68*, *sim4-193*, and double mutants grown on YE5S for 4 d (25°C) or 3 d (30°C). (D) Kinetochore localization of a Fta2-GFP fusion protein in the indicated ts strains. All strains were incubated for 6 h at the nonpermissive temperature before fixation. Wt, wild-type; ++, wild-type–like localization to −, no localization. N/strain = 140. (E) Diagrammatic representation of Fta2-GFP kinetochore localization in *sim4-193* and *mis6-302* cell populations. N/strain = 140. (F) Kinetochore localization of Sim4-GFP, Mis6-HA in a *fta2-291* mutant and Dad1-GFP in a *fta2-292* mutant grown for 6 h at the restrictive temperature. ++, wild-type–like localization to −, no localization. N/strain = 140. (G) Dad1-GFP localization was analyzed in living *fta2-292* cells grown at 25 or 36°C for 6 h.

Extra Mal2 Can Suppress the fta2 ts Mutant Phenotypes

Because *fta2*$^+$ was isolated as a suppressor of the *mal2-1* mutant phenotypes, it was of interest to see whether extra *mal2*$^+$ could suppress the *fta2* mutant phenotypes. *mal2*$^+$ driven by its own promoter on plasmid pUR19 rescued the ts phenotype of the *fta2-292* strain at all temperatures tested (Figure 4A, left), whereas it could only rescue the ts phenotype of the *fta2-291* strain up to 34°C. However overexpression of *mal2*$^+$ from the repressible, wild-type *nmt1*$^+$ promoter resulted in suppression of the *fta2-291* nongrowth phenotype at all temperatures tested (Figure 4A, right). Thus, suppression of the *fta2* ts phenotype by *mal2*$^+$ occurs in the same dosage-dependent manner as has been observed for the suppression of *mal2-1* by *fta2*$^+$. It was therefore not surprising that the kinetochore localization of a Mal2-GFP fusion protein was affected in *fta2* mutants (Figure 4B). The kinetochore association of Mal2-GFP was not affected in *fta2* mutants grown at the permissive temperature, but it was reduced severely in *fta2* ts cells incubated at the restrictive temperature (Figure 4B). Mal2-GFP protein levels were not affected in *fta2* mutant strains incubated at the restrictive temperature (Supplemental Figure 4).

Given the close genetic interaction between *mal2*$^+$ and *fta2*$^+$, we investigated whether the Mal2 and Fta2 proteins interacted. For this purpose, we tested whether HA-tagged Fta2 could be coimmunoprecipitated by GFP-tagged Mal2. Immunoprecipitation with anti-HA or anti-GFP antibodies was carried out with protein extracts from strains that expressed endogenous Fta2-HA and/or Mal2-GFP. We found that Mal2-GFP strongly coimmunoprecipitated Fta2-GFP.

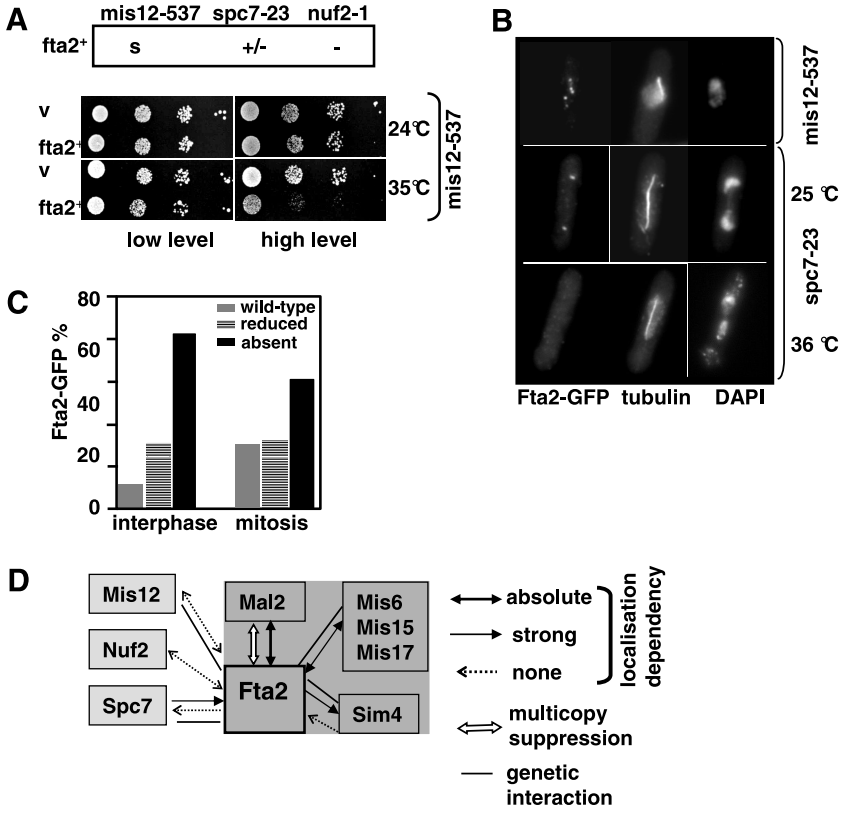

Figure 6. Interaction of *fta2*$^+$ with components of the Ndc80–MIND–Spc7–kinetochore complex. (A) Growth phenotype of *mis12-537*, *spc7-23*, and *nuf2–1* strains transformed with pREPfta2$^+$. s, reduced growth; +/−, slightly reduced growth; −, no effect. The serial dilution patch tests (10^4 to 10^1 cells) show a *mis12-537* strain transformed with pREPfta2$^+$ grown under selective conditions and under *nmt1*$^+$ promoter repressing (low) or derepressing (high) conditions for 6 d. (B) Photomicrographs of *mis12-537* and *spc7-23* cells expressing Fta2-GFP. The *spc7-23* strain was incubated at 25°C or for 6 h at 36°C, the *mis12-537* strain for 6 h at 36°C, fixed, and stained with DAPI, anti-tubulin antibody, and anti-GFP antibody. Bar, 5 μm. (C) Diagrammatic representation of Fta2-GFP in a *spc7-23* cell population incubated for 6 h at 36°C. N/cell cycle phase, 55. (D) Summary of the interactions between Fta2 and components of the Sim4 and Ndc80–MIND–Spc7 complexes.

Fta2-HA could also coimmunoprecipitate Mal2-GFP (Supplemental Figure 3).

Given the close physical and genetic interaction between *fta2*$^+$ and *mal2*$^+$, we were interested to analyze the phenotype of *fta2 mal2* double mutants. However, we were unable to construct *mal2-1 fta2-291* or *mal2-1 fta2-292* mutants by tetrad analysis at 25°C. The *mal2-1 fta2* double mutant spores germinated, and cells divided two to three times before dying (see *Materials and Methods*).

Interaction between Fta2 and Other Components of the Sim4 Kinetochore Subcomplex

Recently, Fta2 and Mal2 were identified as components of the Sim4 kinetochore complex (Liu *et al*., 2005). The Sim4 complex consists of the previously identified proteins Sim4, Mal2, Mis6, Mis15, and Mis17; the DASH component Dad1; and seven novel proteins, Fta1-7 (Goshima *et al*., 1999; Jin *et al*., 2002; Pidoux *et al*., 2003; Hayashi *et al*., 2004; Liu *et al*., 2005). Given the close interaction between Mal2 and Fta2 for all parameters tested, we assayed the interaction between Fta2 and other components of the Sim4 complex. We first tested suppression of all existing conditional lethal alleles of the Sim4 complex components by overexpression of *fta2*$^+$. *fta2*$^+$ expressed from the repressible, wild-type *nmt1*$^+$ promoter was unable to suppress the nongrowth phenotype of the ts *sim4-193*, *mis6-302*, *mis15-68*, or *mis17-362* strains even at semipermissive temperatures (Figure 5A). In fact, overexpression of *fta2*$^+$ in *mis6-302* was synthetic lethal at 31°C, a temperature that has only a slight effect on the growth of the *mis6* mutant transformed with a vector control (Figure 5A).

Next, double mutants of *fta2-291* and/or *fta2-292* with *sim4-193*, *mis6-302*, *mis15-68* were constructed by tetrad analysis. In contrast to the *fta2 mal2-1* double mutants, which were inviable, all of these double mutants were able to grow normally at 25°C. However, at higher temperatures, synthetic effects were observed that resulted in poor growth at that particular temperature (Figure 5B). As an example, single and double mutant strains of *fta2-291* and *mis15-68* and *sim4-193* are shown (Figure 5C). To determine whether kinetochore localization of Fta2 was affected in mutants of the Sim4 complex, we assayed localization of a Fta2-GFP fusion protein in *sim4-193*, *mis6-302*, *mis15-68*, and *mis17-262* mutants. At the permissive temperature (25°C), no difference in Fta2-GFP staining was observed between a wild-type strain and the Sim4 complex mutants, with the exception of the *mal2-1* mutant, which showed less intense Fta2-GFP signals (Figure 5D; our unpublished data). At the nonpermissive temperature, no Fta2-GFP signal was observed in *mal2-1* cells (Figure 2B), and severely reduced signals were observed in *mis6-302*, *mis15-68*, and *mis17-362* cells (Figure 5D). For example, only 10% of *mis6-302* cells incubated for 6 h at 36°C showed a wild-type–like Fta2-GFP signal; all other cells had a severely reduced or no GFP signal (Figure 5E). This phenotype was irrespective of the cell cycle phase, although interphase cells showed a higher percentage of cells with no GFP signal/versus reduced signal than mitotic cells. Analysis of a Mis6-HA fusion protein in the *fta2-291* mutant gave a similar result (Figure 5F).

Surprisingly, the presence of the mutant *sim4* allele had only mild effects on the correct localization of Fta2-GFP. After 6–8 h at the restrictive temperature, 86% of *sim4-193* cells showed wild-type–like Fta2-GFP signals (Figure 5E). However, the correct localization of a Sim4-GFP fusion protein was dependent on Fta2, because kinetochore localization of Sim4-GFP in the *fta2-291* mutant was reduced severely (Figure 5F; our unpublished data).

These results imply that the Sim4 kinetochore complex is build up hierarchically. Mal2 is absolutely required for ki-

netochore localization of Fta2. Mis6, Mis15, and Mis17 are also needed for Fta2 localization, but to a somewhat lesser degree, whereas Sim4 does not seem to be required. Fta2 is absolutely required for kinetochore localization of Mal2 and plays an important role in the correct localization of Mis6 and Sim4 proteins.

Finally, it has been shown previously that Sim4 complex components are required for association of the DASH complex (Sanchez-Perez *et al.*, 2005). We therefore tested whether Dad1, a constitutive component of the DASH complex was localized correctly in *fta2-292* mutant cells and found that kinetochore localization of Dad1-GFP was dependent on functional *fta2*$^+$ (Figure 5, F and G).

Wild-Type–like Fta2 Localization Requires Spc7, a Component of the Ndc80–MIND–Spc7 Kinetochore Complex

Recently, the Ndc80–MIND–Spc7 kinetochore complex has been described (Obuse *et al.*, 2004; Liu *et al.*, 2005). This complex seems to exist independently of the Sim4 complex (Liu *et al.*, 2005).

To analyze a possible interaction between Fta2 and components of the Ndc80–MIND–Spc7 complex, we overexpressed *fta2*$^+$ in *mis12-537*, *nuf2-1*, and *spc7-23* mutant strains at various temperatures up to the maximally permissive temperatures. The Mis12 protein is part of the MIND complex, whereas Nuf2 is a component of the Ndc80 complex. Extra *fta2*$^+$ had no effect on the growth of a *nuf2–1* mutant, a slight negative effect on the *spc7-23* mutant and gave rise to reduced growth of the *mis12-537* mutant strain (Figure 6A).

To test whether Fta2 kinetochore localization was dependent on the Ndc80–MIND–Spc7 complex, subcellular localization of the Fta2-GFP fusion protein was determined in *mis12-537*, *nuf2-1*, and *spc7-23* ts strains (Goshima *et al.*, 1999; Nabetani *et al.*, 2001; Kerres *et al.*, 2004). Kinetochore localization of Fta2-GFP was unaffected in *mis12-537* and *nuf2-1* mutant strains incubated at the nonpermissive temperature (Figure 6B; our unpublished data). However, surprisingly, Fta2-GFP localization was affected in the *spc7-23* strain at the restrictive temperature (Figure 6B). *spc7-23* encodes a ts mutant Spc7 protein that has a severely reduced kinetochore association at the restrictive temperature, leading to spindle defects and massive chromosome missegregation (Kerres, Jakopec, and Fleig, unpublished data). Whereas Fta2-GFP kinetochore localization was unaffected in a *spc7-23* strain grown at 25°C (Figure 6B), the signal intensity of the fusion protein was reduced or absent in the majority of *spc7-23* cells incubated at the restrictive temperature (Figure 6, B and C). Fta2 proteins levels were similar in *spc7-23* and wild-type cells (Supplemental Figure 1). Thus, Spc7 is required for correct localization of the Sim4 complex component Fta2. However, a Spc7-GFP fusion protein is localized correctly in a *fta2* mutant (our unpublished data).

DISCUSSION

We investigated the role of the conserved Mal2 protein in mitosis by screening for extragenic suppressors that were able to rescue the *mal2-1* ts phenotype at a semipermissive growth temperature and thus identified the essential kinetochore component Fta2. Both proteins were recently shown to be members of the Sim4 kinetochore complex (Liu *et al.*, 2005).

Our characterization of Fta2 shows that it localizes to the central domain of the fission yeast centromere, where it is required for transcriptional silencing. This specific alleviation of central core silencing has also been documented for other mutant components of the Sim4-complex, such as Mis6, Mal2, and Sim4, and probably reflects defects in the assembly of the kinetochore (Allshire *et al.*, 1995; Jin *et al.*, 2002; Pidoux *et al.*, 2003). The ts *fta2* mutants show a very high number of aberrant mitosis with no or unequal separation of the condensed chromatin indicating the important role of Fta2 in kinetochore function. The high frequency of mitotic cells with nonseparated chromatin on an elongating spindle (nearly 50% in the *fta2-291* strain) has so far not been observed for other mutant components of the Sim4 complex and implies that kinetochore function is severely affected in *fta2* mutants.

Analysis of the segregation behavior of tagged *cen1* sister centromeres indicated that Fta2 is required for bipolar chromosome orientation. In addition, 44% of cen1-GFP signals did not seem to be spindle associated in anaphase *fta2* mutants, implying that Fta2 also plays a role in linking the kinetochore to microtubule plus-ends.

The spindle checkpoint monitors spindle–kinetochore interaction and becomes activated when the mitotic chromosomes are not under tension or/and are not microtubule associated (Musacchio and Hardwick, 2002; Cleveland *et al.*, 2003). Given the phenotype of the *fta2* mutants, one would expect activation of the spindle checkpoint in these strains. Indeed, we observed that in the absence of the spindle checkpoint component Mph1, the temperature sensitivity and chromosome missegregation phenotype of a *fta2* mutant strain was increased significantly. However, double mutants between *fta2-291* and *mad2*Δ behaved like the *fta2-291* single mutant. Recently, it has been shown that Mis6 is required for the association of Mad2 with the kinetochore during mitosis (Saitoh *et al.*, 2005). Because the Mis6 protein is not localized correctly in *fta2* mutants, we presume that the Mad2-dependent part of the spindle checkpoint pathway is impaired in *fta2* mutants and thus unable to sense the aberrant microtubule–kinetochore interactions.

Fta2 is a component of the 13-component Sim4 kinetochore complex that comprises the previously identified proteins Mal2, Mis6, Sim4, Mis15, and Mis17; the DASH component Dad1; and the seven new Fta1-7 proteins (Liu *et al.*, 2005). Apart from the nonessential Dad1 protein, all other Sim4 complex components analyzed to date are essential for precise chromosome transmission. However, the phenotypes caused by various mutant alleles coding for Sim4 complex components are not identical (Fleig *et al.*, 1996; Goshima *et al.*, 1999; Jin *et al.*, 2002; Pidoux *et al.*, 2003; Hayashi *et al.*, 2004; Liu *et al.*, 2005; Sanchez-Perez *et al.*, 2005). For example, *mal2-1* and *sim4-193* mutants are hypersensitive to microtubule-destabilizing drugs, whereas others, such as *mis6-302* or *fta2* mutants, are not (Jin *et al.*, 2002; Pidoux *et al.*, 2003; our unpublished data). By analyzing the interactions between Fta2 and other members of the Sim4 complex, we have started to identify functional subgroups within this complex (Figure 6F). In particular, the tight functional interaction with Mal2 was not observed for other members of this complex. *mal2*$^+$ overexpression strongly suppressed the ts phenotype of the *fta2* mutants in a dosage-dependent manner. The same held true for the rescue of the *mal2-1* ts phenotype by extra *fta2*$^+$. Furthermore, kinetochore localization of these proteins was absolutely dependent on each other. These data imply that Mal2 and Fta2 work together in a subgroup of the Sim4 complex. Because *fta2 mal2-1* double mutants could not be obtained at any temperature, *fta2* and *mal2* mutants require the presence of the other wild-type partner protein for survival at the permissive temperature.

Such a close functional interaction has not been observed for any other members of the Sim4 complex. For example, all double mutants of essential Sim4 complex components generated to date were viable at the permissive temperature (22–26°C) and showed growth impairment only at higher temperatures (Pidoux *et al*., 2003; Hayashi *et al*., 2004) (Figure 5B).

Furthermore, reciprocal suppression has not yet been observed for any other members of the Sim4 complex. Although Mis6, Mis17, and Mis15 proteins show strong coimmunoprecipitation and depend on each other for correct kinetochore localization, they show no suppression of each others mutant phenotype (Hayashi *et al*., 2004). Extra Sim4 protein is able to rescue the ts phenotype of a *mis6-302* mutant; however, the converse is not true (Pidoux *et al*., 2003). We have shown that *fta2*$^+$ or *mal2*$^+$ overexpression did not rescue the ts phenotype of *sim4-193*, *mis15-68*, and *mis17-362* mutant strains and that extra *fta2*$^+$ in the *mis6-302* mutant gave rise to a synthetic lethal phenotype. Interestingly, *gfp*-tagged *fta2*$^+$ in *mis17-365* and *mis15-68* but not other Sim4 component strains resulted in an increased ts sensitivity of these strains (our unpublished data), possibly implying that Fta2 and Mis17/Mis15 are in proximity to each other.

Kinetochore localization of Fta2 was absolutely dependent on Mal2; strongly dependent on functional Mis15, Mis17, and Mis6 proteins; but unaffected in *sim4* mutant cells, implying that the Sim4 complex is build up in a hierarchical manner (Figure 6F).

Interestingly, we found that wild-type–like kinetochore localization of Fta2 is dependent on the presence of a functional Spc7 protein. Spc7, which was isolated as a suppressor of the EB1 family member Mal3 and plays a role at the microtubule–kinetochore interface, is closely associated with the Ndc80 and MIND complexes (Kerres *et al*., 2004; Obuse *et al*., 2004; Liu *et al*., 2005). Our data thus indicate an interaction between the Ndc80–MIND–Spc7 and Sim4 complexes, which is possibly mediated via Spc7 and Fta2. The functional significance of this interaction awaits further analysis; however, given the finding that Spc7 associates with the microtubule plus-end–associating protein Mal3 and that the Sim4 complex Fta2 is required for kinetochore association of the DASH complex, it is possible that this interaction contributes to the dynamic microtubule–kinetochore interface.

ACKNOWLEDGMENTS

We thank M. Yanagida, Y. Hiraoka, J. Millar, S. Sazer, and K. Gould for strains; E. Walla for excellent technical assistance; J. Hegemann for support; and K. Gull for the anti-tubulin antibody TAT1. The initial stages of this work were supported by funds from the Deutsche Forschungsgemeinschaft (to U.F.)

REFERENCES

Allshire, R. C., Javerzat, J. P., Redhead, N. J., and Cranston, G. (1994). Position effect variegation at fission yeast centromeres. Cell *76*, 157–169.

Allshire, R. C., Nimmo, E. R., Ekwall, K., Javerzat, J. P., and Cranston, G. (1995). Mutations derepressing silent centromeric domains in fission yeast disrupt chromosome segregation. Genes Dev. *9*, 218–233.

Altschul, S. F., Madden, T. L., Schaffer, A. A., Zhang, J., Zhang, Z., Miller, W., and Lipman, D. J. (1997). Gapped BLAST and PSI-BLAST: a new generation of protein database search programs. Nucleic Acids Res. *25*, 3389–3402.

Bahler, J., Wu, J. Q., Longtine, M. S., Shah, N. G., McKenzie, A., 3rd, Steever, A. B., Wach, A., Philippsen, P., and Pringle, J. R. (1998). Heterologous modules for efficient and versatile PCR-based gene targeting in *Schizosaccharomyces pombe*. Yeast *14*, 943–951.

Barbet, N., Muriel, W. J., and Carr, A. M. (1992). Versatile shuttle vectors and genomic libraries for use with *Schizosaccharomyces pombe*. Gene *114*, 59–66.

Bridge, A. J., Morphew, M., Bartlett, R., and Hagan, I. M. (1998). The fission yeast SPB component Cut12 links bipolar spindle formation to mitotic control. Genes Dev. *12*, 927–942.

Cleveland, D. W., Mao, Y., and Sullivan, K. F. (2003). Centromeres and kinetochores: from epigenetics to mitotic checkpoint signaling. Cell *112*, 407–421.

De Wulf, P., McAinsh, A. D., and Sorger, P. K. (2003). Hierarchical assembly of the budding yeast kinetochore from multiple subcomplexes. Genes Dev. *17*, 2902–2921.

Desai, A., Rybina, S., Muller-Reichert, T., Shevchenko, A., Hyman, A., and Oegema, K. (2003). KNL-1 directs assembly of the microtubule-binding interface of the kinetochore in *C. elegans*. Genes Dev. *17*, 2421–2435.

Doheny, K. F., Sorger, P. K., Hyman, A. A., Tugendreich, S., Spencer, F., and Hieter, P. (1993). Identification of essential components of the *S. cerevisiae* kinetochore. Cell *73*, 761–774.

Fleig, U., Sen-Gupta, M., and Hegemann, J. H. (1996). Fission yeast mal2+ is required for chromosome segregation. Mol. Cell. Biol. *16*, 6169–6177.

Foltz, D. R., Jansen, L. E., Black, B. E., Bailey, A. O., Yates, J. R., 3rd, and Cleveland, D. W. (2006). The human CENP-A centromeric nucleosome-associated complex. Nat. Cell Biol. *8*, 458–469.

Fukagawa, T. (2004). Centromere DNA, proteins and kinetochore assembly in vertebrate cells. Chromosome Res. *12*, 557–567.

Goshima, G., Saitoh, S., and Yanagida, M. (1999). Proper metaphase spindle length is determined by centromere proteins Mis12 and Mis6 required for faithful chromosome segregation. Genes Dev. *13*, 1664–1677.

Hagan, I. M., and Hyams, J. S. (1988). The use of cell division cycle mutants to investigate the control of microtubule distribution in the fission yeast *Schizosaccharomyces pombe*. J. Cell Sci. *89*, 343–357.

Hayashi, T., Fujita, Y., Iwasaki, O., Adachi, Y., Takahashi, K., and Yanagida, M. (2004). Mis16 and Mis18 are required for CENP-A loading and histone deacetylation at centromeres. Cell *118*, 715–729.

He, X., Jones, M. H., Winey, M., and Sazer, S. (1998). Mph1, a member of the Mps1-like family of dual specificity protein kinases, is required for the spindle checkpoint in *S. pombe*. J. Cell Sci. *111*, 1635–1647.

He, X., Patterson, T. E., and Sazer, S. (1997). The *Schizosaccharomyces pombe* spindle checkpoint protein mad2p blocks anaphase and genetically interacts with the anaphase-promoting complex. Proc. Natl. Acad. Sci. USA *94*, 7965–7970.

He, X., Rines, D. R., Espelin, C. W., and Sorger, P. K. (2001). Molecular analysis of kinetochore-microtubule attachment in budding yeast. Cell *106*, 195–206.

Janke, C., Ortiz, J., Lechner, J., Shevchenko, A., Magiera, M. M., Schramm, C., and Schiebel, E. (2001). The budding yeast proteins Spc24p and Spc25p interact with Ndc80p and Nuf2p at the kinetochore and are important for kinetochore clustering and checkpoint control. EMBO J. *20*, 777–791.

Jin, Q. W., Pidoux, A. L., Decker, C., Allshire, R. C., and Fleig, U. (2002). The mal2p protein is an essential component of the fission yeast centromere. Mol. Cell. Biol. *22*, 7168–7183.

Kerres, A., Vietmeier-Decker, C., Ortiz, J., Karig, I., Beuter, C., Hegemann, J., Lechner, J., and Fleig, U. (2004). The fission yeast kinetochore component Spc7 associates with the EB1 family member Mal3 and is required for kinetochore-spindle association. Mol. Biol. Cell *15*, 5255–5267.

Liu, X., McLeod, I., Anderson, S., Yates, J. R., 3rd, and He, X. (2005). Molecular analysis of kinetochore architecture in fission yeast. EMBO J. *24*, 2919–2930.

Maiato, H., DeLuca, J., Salmon, E. D., and Earnshaw, W. C. (2004). The dynamic kinetochore-microtubule interface. J. Cell Sci. *117*, 5461–5477.

McAinsh, A. D., Tytell, J. D., and Sorger, P. K. (2003). Structure, function, and regulation of budding yeast kinetochores. Annu. Rev. Cell Dev. Biol. *19*, 519–539.

Meraldi, P., McAinsh, A. D., Rheinbay, E., and Sorger, P. K. (2006). Phylogenetic and structural analysis of centromeric DNA and kinetochore proteins. Genome Biol. *7*, R23.

Moreno, S., Klar, A., and Nurse, P. (1991). Molecular genetic analysis of fission yeast *Schizosaccharomyces pombe*. Methods Enzymol. *194*, 795–823.

Musacchio, A., and Hardwick, K. G. (2002). The spindle checkpoint: structural insights into dynamic signalling. Nat Rev. Mol. Cell Biol. *3*, 731–741.

Nabeshima, K., Nakagawa, T., Straight, A. F., Murray, A., Chikashige, Y., Yamashita, Y. M., Hiraoka, Y., and Yanagida, M. (1998). Dynamics of centromeres during metaphase-anaphase transition in fission yeast: Dis1 is impli-

cated in force balance in metaphase bipolar spindle. Mol. Biol. Cell *9*, 3211–3225.

Nabetani, A., Koujin, T., Tsutsumi, C., Haraguchi, T., and Hiraoka, Y. (2001). A conserved protein, Nuf2, is implicated in connecting the centromere to the spindle during chromosome segregation: a link between the kinetochore function and the spindle checkpoint. Chromosoma *110*, 322–334.

Obuse, C., Iwasaki, O., Kiyomitsu, T., Goshima, G., Toyoda, Y., and Yanagida, M. (2004). A conserved Mis12 centromere complex is linked to heterochromatic HP1 and outer kinetochore protein Zwint-1. Nat. Cell Biol. *6*, 1135–1141.

Okada, M., Cheeseman, I. M., Hori, T., Okawa, K., McLeod, I. X., Yates, J. R., Desai, A., and Fukagawa, T. (2006). The CENP-H-I complex is required for the efficient incorporation of newly synthesized CENP-A into centromeres. Nat. Cell Biol. *5*, 446–457.

Ortiz, J., Stemmann, O., Rank, S., and Lechner, J. (1999). A putative protein complex consisting of Ctf19, Mcm21, and Okp1 represents a missing link in the budding yeast kinetochore. Genes Dev. *13*, 1140–1155.

Partridge, J. F., Borgstrom, B., and Allshire, R. C. (2000). Distinct protein interaction domains and protein spreading in a complex centromere. Genes Dev. *14*, 783–791.

Pidoux, A. L., and Allshire, R. C. (2000). Centromeres: getting a grip of chromosomes. Curr. Opin. Cell Biol. *12*, 308–319.

Pidoux, A. L., and Allshire, R. C. (2004). Kinetochore and heterochromatin domains of the fission yeast centromere. Chromosome Res. *12*, 521–534.

Pidoux, A. L., Richardson, W., and Allshire, R. C. (2003). Sim *4*, a novel fission yeast kinetochore protein required for centromeric silencing and chromosome segregation. J. Cell Biol. *161*, 295–307.

Polizzi, C., and Clarke, L. (1991). The chromatin structure of centromeres from fission yeast: differentiation of the central core that correlates with function. J. Cell Biol. *112*, 191–201.

Russell, I. D., Grancell, A. S., and Sorger, P. K. (1999). The unstable F-box protein p58-Ctf13 forms the structural core of the CBF3 kinetochore complex. J. Cell Biol. *145*, 933–950.

Saitoh, S., Ishii, K., Kobayashi, Y., and Takahashi, K. (2005). Spindle checkpoint signaling requires the mis6 kinetochore subcomplex, which interacts with mad2 and mitotic spindles. Mol. Biol. Cell *16*, 3666–3677.

Saitoh, S., Takahashi, K., and Yanagida, M. (1997). Mis6, a fission yeast inner centromere protein, acts during G1/S and forms specialized chromatin required for equal segregation. Cell *90*, 131–143.

Sanchez-Perez, I., Renwick, S. J., Crawley, K., Karig, I., Buck, V., Meadows, J. C., Franco-Sanchez, A., Fleig, U., Toda, T., and Millar, J. B. (2005). The DASH complex and Klp5/Klp6 kinesin coordinate bipolar chromosome attachment in fission yeast. EMBO J. *24*, 2931–2943.

Takahashi, K., Chen, E. S., and Yanagida, M. (2000). Requirement of Mis6 centromere connector for localizing a CENP-A-like protein in fission yeast. Science *288*, 2215–2219.

Takahashi, K., Murakami, S., Chikashige, Y., Funabiki, H., Niwa, O., and Yanagida, M. (1992). A low copy number central sequence with strict symmetry and unusual chromatin structure in fission yeast centromere. Mol. Biol. Cell *3*, 819–835.

Westermann, S., Cheeseman, I. M., Anderson, S., Yates, J. R., 3rd, Drubin, D. G., and Barnes, G. (2003). Architecture of the budding yeast kinetochore reveals a conserved molecular core. J. Cell Biol. *163*, 215–222.

Wigge, P. A., and Kilmartin, J. V. (2001). The Ndc80p complex from *Saccharomyces cerevisiae* contains conserved centromere component and has a function in chromosome segregation. J. Cell Biol. *152*, 349–360.

Winey, M., Mamay, C. L., O'Toole, E. T., Mastronarde, D. N., Giddings, T. H., Jr., McDonald, K. L., and McIntosh, J. R. (1995). Three-dimensional ultrastructural analysis of the *Saccharomyces cerevisiae* mitotic spindle. J. Cell Biol. *129*, 1601–1615.